using for K_s, the shape factor, Witham's value of about 0.5 for a slender projectile and for K_r, the reflection coefficient, a value of 2. For the rocket dimensions, D (diameter) is 10 m, L (length) is 68.5 m, and K_sD/L is 0.073. With these values Δp is computed to be 0.1 μb (0.1 dyne/cm^2) rather than the observed signal, which is two orders of magnitude larger.

But the effective cross section of the rocket is much larger than the cross section of the rocket itself as a result of the spreading of the rocket's exhaust gas. The exhaust plume travels with the rocket and serves as a blunt body of large cross section moving at supersonic speed through the ambient air, thus generating a shock much stronger than that which would come from the rocket casing alone. The effective width (D) of the source is certainly much greater than the simple diameter of the casing, as is the case with supersonic aircraft (*6*). Reasonable values of the plume diameter can increase the value of K_sD/L to the order of 10, thus giving the observed Δp. However, the Witham formula does not include attenuation terms because prior applications of the formula have been to low-elevation supersonic objects where attenuation is relatively small. Moreover, the complete explanation involves consideration of the effect of drag.

As we noted above, during propagation through the upper atmosphere a sonic wave with a period of about 1 second would be severely attenuated. But the presence of the recorded signals and calculations of the signal strength at high elevations require that the sonic wave propagate as a shock front through the rarefied upper atmosphere. In order to explain this observation, we must assume that the nonlinear propagation of a shock front at these elevations must occur with much lower damping than for an acoustic wave. Only when the wave approaches a few tens of kilometers above the surface does its amplitude become small enough for acoustic damping to apply, but at this elevation the kinematic viscosity is sufficiently low so that the attenuation there is negligible. Thus, the recorded signals, which at first seemed unlikely, appear tractable.

DONALD COTTEN*
WILLIAM L. DONN†
Lamont-Doherty Geological Observatory, Columbia University, Palisades of New York 10964

References and Notes

1. G. Kaschak, W. Donn, U. Fehr, *J. Acoust. Soc. Amer.* **48**, 12 (1970).
2. U. Fehr, *ibid.* **42**, 991 (1967).
3. F. G. Finger and R. M. McInturff, *Science* **167**, 16 (1970).
4. D. Cotten and W. L. Donn, in preparation.
5. R. Courant and K. Friedrichs, *Supersonic Flow and Shock Waves* (Interscience, New York, 1948), p. 165.
6. H. Carlson, R. Mack, O. Morris, *J. Acoust. Soc. Amer.* **39**, part 2, S10 (1966).
7. H. Grad, "Aerodynamics of the Upper Atmosphere," *Rand Rep. R-339* (1959), p. 11-1.
8. G. Witham, *Proc. Roy. Soc. Ser. A Math. Phys. Sci.* **201**, 89 (1950).
9. A. Pierce and C. Thomas, *J. Acoust. Soc. Amer.* **46**, 1366 (1969).
10. We are grateful to C. Hartdegen, P. Inman, J. Laudadio, and B. Patterson of the Columbia Geophysical Station in Bermuda and D. Wolf of the Lamont-Doherty Geophysical Observatory for invaluable assistance in the field. This work was made possible by NSF grants GA 1333 and 17454 and U.S. Army Electronics Command and U.S. Army Research Office Durham contracts DAAB-07-69-C-0250 and DAHC 04-67-C-0037, respectively. Lamont-Doherty Geological Observatory (Columbia University) Contribution No. 1618.

* Also on the faculty of Queensborough Community College of the City University of New York.

† Also on the faculty of the City College of the City University of New York.

19 October 1970

■

Alteration of Lunar Optical Properties: Age and Composition Effects

Abstract. *A model for lunar surface processes is presented which explains the main albedo and color contrasts and the temporal changes in these optical properties. Evidence from Apollo 11 and Apollo 12 samples and telescopic spectral reflectivity measurements indicates that the maria are similar in mineralogy on a regional scale and that the highlands are consistent with an anorthositic-gabbro composition. Bright craters and rays in both regions expose materials that are relatively crystalline compared with their backgrounds, which are richer in dark glass. With age, bright craters and rays in the maria darken in place by meteorite impact–induced vitrification and mixing with the surrounding material. Highland bright craters and rays may, however, darken primarily through regional contamination by iron- and titanium-rich mare material.*

We have previously compared the spectral reflectivity (0.35 to 2.5 μm) of the Apollo 11 surface fines with telescopic data for an area 18 km in diameter containing the landing site (*1*, *2*). The very close agreement between sample measurements and telescopic measurements implies that the Apollo 11 surface fines are representative of areas of 10-km scale or larger. It was also possible to show that the optical properties of the samples are a function of the mineralogy and the glass content.

Recently we have measured spectral-reflectivity curves for Apollo 12 samples from Oceanus Procellarum. We have compared these curves with the Apollo 11 sample data and with a variety of telescopic measurements for the near side of the moon. Comparison of the several sample curves and the telescope curves has led to new conclusions about the composition of the lunar surface as a whole and about surface processes.

Laboratory measurements were made with a Beckman DK-2A ratio-recording spectrophotometer over the spectral range of 0.35 to 2.5 μm. The instrumentation and the sample-handling techniques are discussed elsewhere (*2*).

Comparison of spectral-reflectivity curves of the Apollo 12 fines and the Apollo 11 fines reveals (*3*):

1) Two Apollo 12 samples of bulk fines (samples 12042 and 12070) and two samples from near the top of the double core tube (samples 12025,13 and 12025,6) have essentially identical reflectivity curves. These samples will be referred to as "surface fines."

2) The Apollo 12 surface fines have an integral reflectivity that is 10 percent higher than the Apollo 11 surface fines in the visible spectral region (0.4 to 0.7 μm).

3) The slope of the curve for the Apollo 11 surface fines is less steep than that for the Apollo 12 surface fines.

4) The Apollo 12 surface fines show a 6 percent deeper absorption band at 0.95 μm than does the Apollo 11 material and the Apollo 12 curve contains a second broad band at 2.0 μm that the Apollo 11 curve does not have.

5) Material that is 20 cm below the top of the Apollo 12 core tube has an integral reflectivity in the visible range that is 40 percent higher than is this value for the Apollo 12 surface fines.

6) The curve slope is less steep and the 0.95- and 2.0-μm bands are deeper for the 20-cm-deep sample from Apollo 12 than for the surface samples.

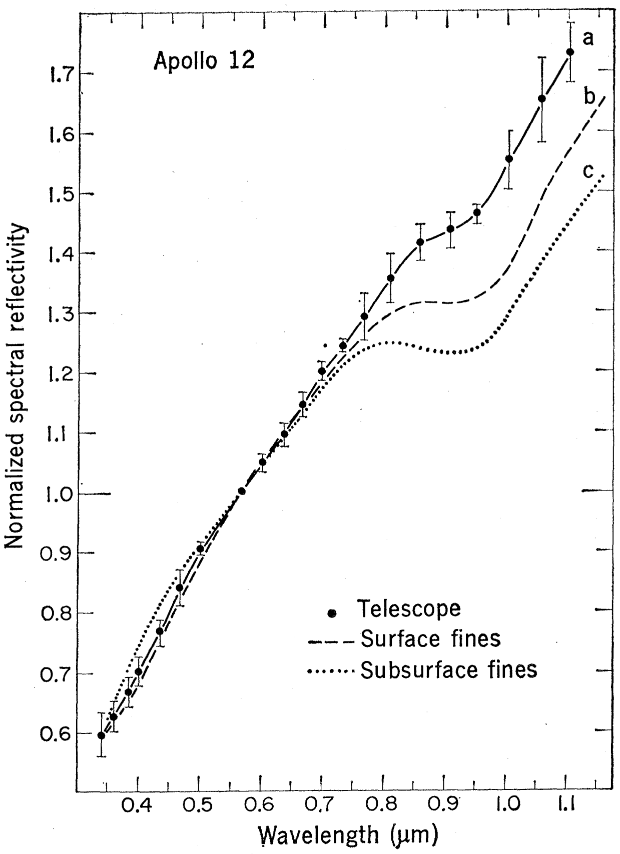

Fig. 1. Comparison of the spectral reflectivity (scaled to unity at 0.56 μm) of Apollo 12 soil samples, taken at the surface (*b*) and at about 20 cm depth (*c*) in the core tube, and telescopic measurements (*10, 11*) of an area approximately 18 km in diameter containing the Apollo 12 site (*a*).

It has been proposed (*1, 2, 4, 5*) that the abundant dark glass accounts for the low reflectivity and the steep curve of the Apollo 11 fines. We have previously shown (*2*) the progressive masking of the 0.95- and 2.0-μm pyroxene absorption bands and the steepening of the curves, from crystalline rock to breccia and to fines. We concluded that impact melting of ilmenite-rich rocks and dissolution of the strongly absorbing Fe and Ti ions account for the dark brown color of the glass. This conclusion was also reached by Conel and Nash (*4*), who fused Apollo 11 crystalline rock and observed a reduction in albedo of over one half and a steepening of the curve comparable to the curve observed for the glassy fines.

Others (*6*) have suggested that solar-wind bombardment has deposited metal coatings on lunar soil particles and that these account for the low albedo of the moon. However, we and others (*7*) find that metal coatings on soil particles are very rare in both Apollo 11 and Apollo 12 samples, and the few visible coatings that do exist are primarily impact-splashed meteoritic and indigenous metals (*8*) and are not due to sputtering. Our laboratory results indicate little or no effect on the bulk optical properties of the lunar surface by metals.

We explain the differences among the curves for the Apollo 11 and Apollo 12 fines as being controlled primarily by the amount of (dark) glass that is present. The more mature Apollo 11 soil contains 50 percent glass (*9*); Apollo 12 surface fines contain 20 percent glass (*9*); and we estimate that the 20-cm-deep sample from Apollo 12 contains 10 percent glass. The chemical composition of these fines is similar, although Ti is a factor of 2 lower in Apollo 12 surface fines than it is in the Apollo 11 fines (*9*).

On the basis of our experience with Apollo 11 (*1, 2*), we expected a very close match between the normalized curves for the Apollo 12 surface fines and the telescopic curve (*10, 11*) for the Apollo 12 landing area. Figure 1 reveals a similarity in curves, but there is a 12 percent difference in the red spectral region, which we consider to be well outside experimental error.

It is known (*9*) that the Apollo 12 site is on a ray of relatively bright material, perhaps associated with the crater Copernicus, which is 370 km to the north. The area around the landing site, approximately 18 km in diameter, measured by means of telescopes, includes mostly darker mare (Fig. 2). The area clearly is more heterogeneous photometrically than is the Apollo 11 site. We conclude that the Apollo 12 surface fines are not representative of the area measured by telescope and that the Apollo 12 sample contains more of the brighter ray material.

We have tested this idea by plotting the ratio of the Apollo 11 telescopically measured reflectivity curve to the Apollo 12 telescopically measured reflectivity curve, and the ratio of the reflectivity curve of Apollo 12 surface fines to the Apollo 12 telescopicially measured reflectivity curve (see Fig. 3). The original telescopic data (*12*) are obtained as ratios of areas to a standard area in Mare Serenitatis. (Knowing the absolute curve for the standard area allows calculation of absolute curves for other areas from the ratios.) The ratio data are accurate to <1 percent, and plots are extremely sensitive to slight changes in the shapes of curves from place to place on the moon (*12*). Earlier studies (*12*) have shown that, on the basis of shape, there are three main classes of ratio curves. Curves are distinct for the ratios for maria to Serenitatis, for uplands to Serenitatis, and for bright craters and rays to Serenitatis. Bright craters can in turn be subdivided into two classes, "young" and "old," on the basis of the ratio curve shape. The curve-type distinction is sharp to the point that an unknown area can be immediately identified when the ratio curve for the area is shown.

The ratio curve for Apollo 11 telescope to Apollo 12 telescope (Fig. 3) is quite similar to that for the "blue" mare to "red" mare class of curves. In other words, the telescope observations of the Apollo 12 site include mostly mare material similar to Mare Serenitatis material (*10, 11*). The ray material at the Apollo 12 site has little effect on the telescopic curve because the area sampled by the telescope observation is large compared with the areas covered by the ray material.

The ratio for Apollo 12 surface fines to Apollo 12 telescope (Fig. 3) shows a curve that is closely similar to curves for "old" bright craters and their rays. The Apollo 12 sample, then, is more raylike than the telescope curve, which includes mostly nonray areas.

The light-toned fines seen at 20 cm

in the Apollo 12 core tube appear to underlie much of the area traversed by the astronauts (*13*). The ratio of 20-cm-deep fines to surface fines yields a curve of the "young" bright crater class (Fig. 3).

The samples studied can therefore be ranked in order of their similarity to telescopic "young" bright crater curves as follows: Apollo 12 fines 20 cm deep; Apollo 12 surface fines; and Apollo 11 surface fines. This is also the order of increasing glass content in otherwise similar materials. We conclude that the ray material differs from the background mare material in that it contains less dark glass. Further, we suggest that bright craters in the maria are, in general, composed of material which is more free of vitreous material and which contains more pulverized crystalline material than the darker mare material.

The darkening of rays with time can then be ascribed to progressive vitrification of the mostly crystalline ray material. Mechanical mixing of ray and darker background material must also occur but is probably less important, except where ray material is very thin. Further evidence to support vitrification as the darkening mechanism is found in the ratio curves (Apollo 12) of surface fines to telescope and of 20-cm-deep fines to telescope (Fig. 3). The two distinctly different ratio curves in Fig. 3 follow the subdivision of telescopic bright-crater curve shapes into those for "young" and "old" craters. The curve for (Apollo 12) surface fines to telescope corresponds in shape to that for "old" bright craters. The curve for 20-cm-deep fines to telescope corresponds to that for the subclass of "young" bright craters. The apparently "fresher" material at depth is similar to the "young" craters, and the glassier (and darker) material at the surface corresponds to the somewhat darkened or "older" bright craters. The dark surface material at the Apollo 12 site can be interpreted as ray material that was darkened in place, rather than as a younger stratigraphic unit.

It seems likely that bright craters in the highlands also expose relatively crystalline material. Information on the mafic silicate phases can be obtained from the absorption bands in the highland bright-crater curves. Interestingly, the bands are at the same frequencies as in the curves for mare crystalline basalts (*11, 14*), which provides strong evidence that clinopyroxene is also the dominant mafic silicate in the highlands.

Wood *et al.* (*15*) have presented evidence that the highlands consist of anorthosite. In the Apollo 11 soil they identified true anorthosite (plagioclase, >90 percent by weight), gabbroic anorthosite (plagioclase, >77 to <90 percent by weight), and anorthositic gabbros (plagioclase, <77 percent by weight).

The true anorthosites contain too little Fe-bearing silicate to give the distinct absorption bands that are seen in the highland bright-crater curves. Further, both the true anorthosites and the gabbroic anorthosites contain olivine as the mafic silicate phase, whereas clinopyroxene is absent or rare (*15*). Olivine produces a single strong band at 1.02 μm and cannot account for the telescopic curves (*16*). The anorthositic gabbro fragments, however, contain clinopyroxene and some olivine as the Fe-silicate phases.

We have separated anorthositic fragments from the Apollo 11 soil and have measured their spectral reflectivity. Although our anorthositic separate contained < 5 percent by weight of mafic minerals, the reflectivity curve has distinct clinopyroxene absorption bands. The bands are at 0.92 and 1.8 μm, which indicates a more pigeonitic pyroxene than is typical for the Apollo 11 and Apollo 12 basalts. This is in agreement with microprobe analyses (*15*) of pyroxenes from the anorthositic rocks.

We conclude that the laboratory and telescopic optical measurements are in general but not precise agreement with the anorthositic model of the highlands.

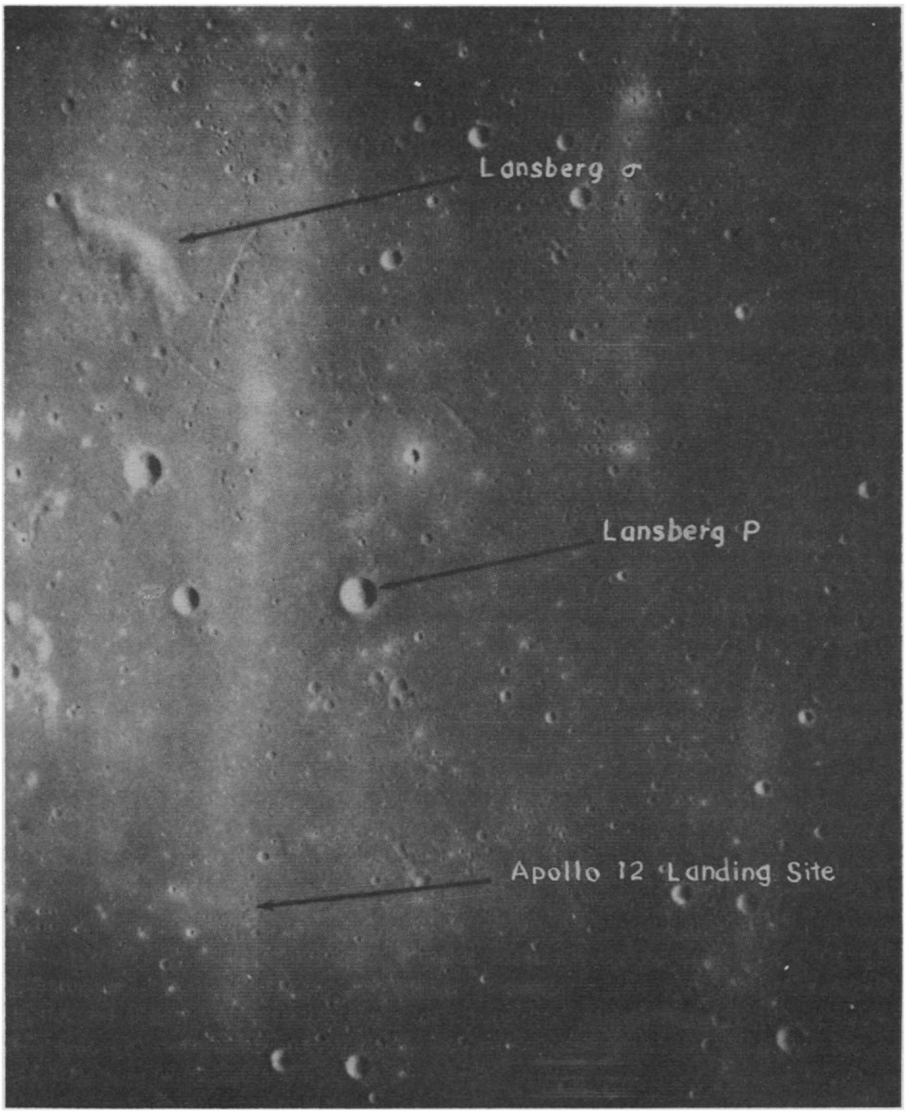

Fig. 2. The Apollo 12 landing area as photographed on the Apollo 11 mission.

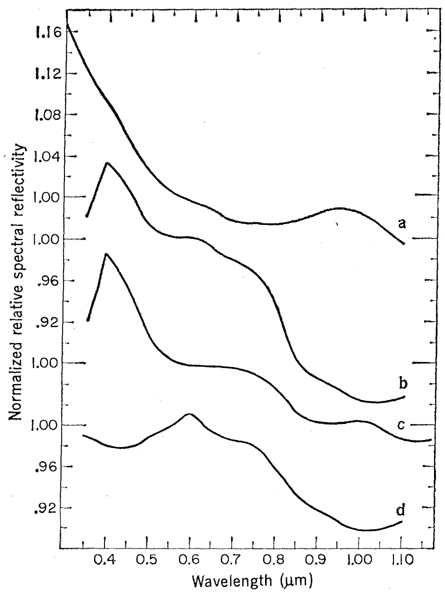

Fig. 3. The ratio of the spectral reflectivities of lunar samples and of the Apollo 11 and Apollo 12 landing areas (~18 km in diameter): (*a*) ratio of Apollo 11 to Apollo 12 area (telescope data); (*b*) ratio of Apollo 12 subsurface to surface soil (laboratory data); (*c*) ratio of Apollo 12 subsurface soil (laboratory data) to Apollo 12 area (telescope data); (*d*) ratio of Apollo 12 surface soil (laboratory data) to Apollo 12 area (telescope data).

The telescopic bands suggest that typical regional highland material, if anorthositic, must be somewhat more gabbroic (more clinopyroxene-rich) than the Apollo 11 anorthositic separate.

Other exotic rocks, such as sample 10085 [Luny Rock 1 (*17*)] and sample 12013 (*9*), are less likely to be representative of the highlands, in terms of their optical properties as they contain calcium-poor pyroxenes. We have not, however, examined these specimens, and we base our conclusions on the inferred reflectivities of their minerals (*3*).

Bright craters and rays in the highlands darken and blend in with the background highland material with time, as occurs in the maria (*11*). With age, the absolute telescopic reflectivity for highland bright craters becomes redder and the absorption bands become weaker, again as in the maria. Darkening does not, however, occur in the highlands to the extent observed in the maria.

We have proposed that impact vitrification produces the darkening and reddening of crystalline material in the maria. Small meteoroid impacts must occur uniformly over the moon. This suggests that the highland curves arise from degradation of bright highland curves as the result of the vitrification process. However, darkening by vitrification requires the presence of ilmenite or other opaques. Whereas the mare soils contain up to 20 percent opaques (mostly ilmenite), the anorthositic crystalline fines contain only a trace of opaques. Glass fragments of anorthositic composition from the Apollo 11 soil lack the steep curve and the strong absorption that is required to mask the pyroxene bands and to match the upland telescopic curves. The question arises then as to how darkening can occur in the highlands if they are anorthositic or if they otherwise lack opaque minerals.

After investigating the reflectivities of glasses made from rocks without opaques (*3*) in the laboratory, we concluded that the only satisfactory reproduction of the "background" highland curves resulted from the simple addition of small quantities of dark glassy fines from mare soil to the anorthositic material. Figure 4 illustrates that contamination by mare fines produces a rapid decrease in reflectivity throughout the spectrum, mainly by coating the larger grains. Significantly, the resulting curves no longer have prominent pyroxene bands, and they match the steepness (redness) of the upland telescope curves. These laboratory results are reported elsewhere in detail (*3*).

It is also possible that on the moon the mare contaminant is predominantly crystalline when added to the uplands; and it is subsequently mixed and darkened through vitrification. (We have not yet tested this more complex model in the laboratory.)

The suggestion that some upland material has contaminated the mare soil is not new (*15, 18*). Wood *et al.* (*15*) proposed on the basis of chemical arguments that upland material makes up approximately 20 percent of the mare soil. They also pointed out the likelihood of the reverse situation—of mare material contaminating the uplands. Our results support this model.

If contamination occurs on a wide scale, an explanation is needed for the apparent sharpness of the mare-highland boundaries. Possible explanations are: (i) Cratering events that splash mare rock onto the highlands will move bright, predominantly crystalline basalt, which will later darken at the surface as mixing and vitrification proceed. The amount of darkening will be limited, however, because the soil will be stirred, exposing highland material. (ii) The highland soil does not become appreciably darker after about 10 percent of dark fines are added (Fig. 4). If all the highlands are contaminated with the equivalent of 10 percent mare-derived dark fines, they will appear everywhere to be closely similar in albedo. (iii) Highland boundary regions typically have a slope. Downhill creep of surface particles (*9*) will tend to continually expose brighter subsurface material on the highland slopes, whereas the surface layer of the flatter maria will accumulate the dark fines produced in situ.

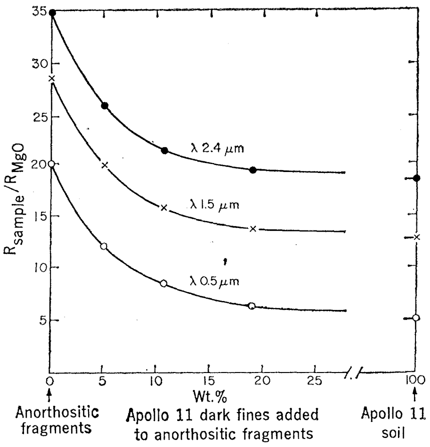

Fig. 4. The change in albedo of anorthositic fragments with addition of Apollo 11 dark surface fines; *R*, reflectivity.

Contamination of the dark mare surfaces by bright highland material should have a more visible albedo effect than the reverse process would. Evidence for such contamination can, in fact, be seen in many parts of the mare regions (for instance, Mare Nectaris). The highland ejecta will be darkened principally through mixing with adjacent and underlying basaltic soil (probably a slower process), which implies that ancient rays of highland material may still be visible on the maria. The lighter maria, then, should in general be older than the darker maria, a conclusion that is in agreement with the geologic evidence.

In summary, we propose the following model: (i) Bright crater material in the maria and in the highlands has a higher ratio of crystal to glass than does the surrounding surface material. (ii) The optical properties of the highlands are consistent with anorthositic gabbro that is contaminated with 5 to

20 percent of darker mare material. (iii) Bright craters and rays in the maria darken and redden in situ by vitrification of the ilmenite-rich basalt (by micrometeoroid impacts) and by mechanical mixing with preexisting dark fines. (iv) Bright craters in the highlands darken largely by the addition of material derived from the maria, which is mixed with highland material and is partially vitrified.

JOHN B. ADAMS
Caribbean Research Institute,
College of the Virgin Islands,
St. Croix 00820

THOMAS B. MCCORD
Planetary Astronomy Laboratory,
Department of Earth and Planetary
Sciences, Massachusetts Institute of
Technology, Cambridge 02139

References and Notes

1. J. B. Adams and R. L. Jones, *Science* **167**, 737 (1970).
2. J. B. Adams and T. B. McCord, in *Proceedings of the Apollo 11 Lunar Science Conference*, A. A. Levinson, Ed. (Pergamon, New York, 1970), vol. 3, p. 1937.
3. ———, in preparation.
4. J. E. Conel and D. B. Nash, in *Proceedings of the Apollo 11 Lunar Science Conference*, A. A. Levinson, Ed. (Pergamon, New York, 1970), vol. 3, p. 2013.
5. D. B. Nash, J. E. Conel, R. T. Greer, *Science* **167**, 721 (1970).

→ T. Gold, M. J. Campbell, B. T. O'Leary, *ibid.*, p. 707; in *Proceedings of the Apollo 11 Lunar Science Conference*, A. A. Levinson, Ed. (Pergamon, New York, 1970), vol. 3, p. 2149; B. W. Hapke, A. J. Cohen, W. A. Cassidy, E. N. Wells, in *ibid.*, p. 2199; B. T. O'Leary and F. Briggs, *J. Geophys. Res.* **75**, 6532 (1970).

7. U. B. Marvin, personal communication.
8. J. I. Goldstein, E. P. Henderson, H. Yakowitz, in *Proceedings of the Apollo 11 Lunar Science Conference*, A. A. Levinson, Ed. (Pergamon, New York, 1970), vol. 1, p. 499; D. S. McKay, W. R. Greenwood, D. A. Morrison, in *ibid.*, p. 673; C. Frondel, C. Klein, Jr., J. Ito, J. C. Drake, in *ibid.*, p. 445; C. L. Herzenberger and D. L. Riley, in *ibid.*, vol. 3, p. 2221; R. M. Housley, M. Blander, M. Abdel-Cadwab, R. W. Grant, A. H. Muir, Jr., in *ibid.*, p. 2251; D. W. Strangway, E. E. Larson, G. W. Pearce, in *ibid.*, p. 2435.
9. See Lunar Sample Preliminary Examination Team [*Science* **165**, 1211 (1969)] for Apollo 11 results; see Lunar Sample Preliminary Examination Team [*ibid.* **167**, 1325 (1970)] for Apollo 12 results.
10. T. V. Johnson and L. A. Soderblom, *J. Geophys. Res.* **74**, 6046 (1969).
11. T. B. McCord, M. Charett, T. V. Johnson, L. Lebofsky, C. Pieters, in preparation.
12. T. B. McCord, *J. Geophys. Res.* **74**, 3131 (1969); ——— and T. V. Johnson, *ibid.*, p. 4395.
13. E. M. Shoemaker *et al.*, in *Apollo 12 Preliminary Science Report, NASA Rep. SP-235* (National Aeronautics and Space Administration, Washington, D.C., 1970), p. 113.
14. T. B. McCord and T. V. Johnson, *Science* **169**, 855 (1970).
15. J. A. Wood, J. S. Dickey, Jr., U. B. Marvin, B. N. Powell, in *Proceedings of the Apollo 11 Lunar Science Conference*, A. A. Levinson, Ed. (Pergamon, New York, 1970), vol. 1, p. 965.
16. J. B. Adams, *Science* **159**, 1453 (1968).

→ A. L. Albee *et al.*, *ibid.* **167**, 463 (1970).

18. E. M. Shoemaker *et al.*, in *Proceedings of the Apollo 11 Lunar Science Conference*, A. A. Levinson, Ed. (Pergamon, New York, 1970), vol. 3, p. 2399.
19. We thank Dr. D. Wones of M.I.T. for invaluable aid in our laboratory vitrification experiments and for many helpful conversations about this manuscript; Drs. J. Wood and U. Marvin of the Smithsonian Astrophysical Observatory and Drs. G. Wasserburg, E. Shoemaker, B. Murry, and L. Silver of Caltech for considerable help in working out our ideas; J. Larsen and C. Gellert of the Caribbean Research Institute for assisting with laboratory measurements; and C. Pieters and M. Charette of M.I.T. for help in handling the telescopic data and in preparing the manuscript. Part of the research described herein was performed while one of us (T.B.M.) was in residence at the Division of Geological Sciences, California Institute of Technology, as a visiting associate. This research was supported by NASA grants and contracts (NGR-22-009-350, NGR-52-083-003, and NAS 9-9478). Contribution 25 of the Planetary Astronomy Laboratory.

11 January 1971

■

The Last Interglacial: Paleotemperatures and Chronology

Abstract. *The* O^{18}/O^{16} *analysis and* Th^{230}/Pa^{231} *dating of deep-sea cores showed that the last interglacial age, with an early major temperature maximum followed by two smaller ones, extended from 100,000 to 70,000 years ago and was preceded by a glacial age extending from 120,000 to 100,000 years ago. The* O^{18}/O^{16} *analysis and* Th^{230}/U^{234} *dating of speleothems confirm and refine these ages.*

The O^{18}/O^{16} analysis of deep-sea cores, together with absolute dating by C^{14} and by methods based on the decay products of the two uranium families, has changed drastically the classical picture of the Pleistocene as given, for instance, by Schuchert and Dunbar (*1*). Not only has postglacial time been reduced to 10,000 years but also the preceding several hundred thousand years have been shown to include rapidly alternating glacial and interglacial events exhibiting an average periodicity of about 50,000 years. High-temperature events in the deep-sea cores were identified by odd integers increasing with time, low-temperature events by even integers (*2*). The amplitude of the temperature oscillations of the surface seawater at low altitudes appears to have increased by about 10 percent toward the present, but age 3, the temperate age preceding the present interglacial, is unique in that it does not exhibit temperatures as high as those of the warm ages before or after [see (*3*) for a possible explanation]. These results were recently reviewed in *Science* (*4*, *5*).

Because temperature did not reach fully interglacial values during age 3, the age closest to us in time which offers conditions most closely resembling the present ones is age 5. Twelve long deep-sea cores from the Atlantic Ocean and adjacent seas have been analyzed so far (*2*, *3*, *6*−*9*), all including stage 5 as well as the adjacent stages 4 and 6. The numerous isotopic curves thus available have been used to reconstruct a detailed generalized isotopic curve from which much of the stratigraphic noise is filtered out (Fig. 1). The time scale is provided by C^{14} and Th^{230}/Pa^{231} measurements (*9*, *10*).

The generalized curve is very characteristic. From stage 7, the curve slopes down to the minimum of stage 6, dated at about 105,000 years before the present. Following a minor inflection, the curve rises rapidly to a major maximum dating from about 95,000 years B.P. This maximum, representing temperatures as high as those of the last hypsithermal, has a duration of only a few thousand years. The isotopic curve then drops to a minimum that is intermediate in value between interglacial maxima and glacial minima. This minimum, dating from about 90,000 years B.P., is followed by a similar minimum about 10,000 years later. Between the two minima and following the second one, the isotopic curve rises, but it reaches only half way up toward the value of the major maximum of 95,000 years B.P. For much of age 5, therefore, temperature was appreciably lower than today. This age came to an end about 70,000 years ago, when temperature began dropping toward the minimum of age 4. This time coincides with the extinction of the pelagic foraminiferal subspecies *Globorotalia menardii flexuosa*. The minimum of age 4 was reached about 10,000 years later, or 60,000 years ago. The characteristic isotopic trend of age 5 was noticed before (*3*) and has been discussed in some detail by Shackleton (*11*), who defined as substages the three isotopic maxima and the two intervening minima occurring within age 5.

The amplitude of the isotopic oscillations within age 5 increases from the Caribbean-equatorial Atlantic to the North Atlantic [core 280, see (*7*)] and the Mediterranean [core 189, see (*6*)].